Cancer Cell
Article

Basal Cell Carcinomas Arise from Hair Follicle Stem Cells in Ptch1$^{+/-}$ Mice

Grace Ying Wang,[1] Joy Wang,[1] Maria-Laura Mancianti,[2] and Ervin H. Epstein, Jr.[1,*]
[1]Children's Hospital Oakland Research Institute, 5700 Martin Luther King Jr. Way, Oakland, CA 94609, USA
[2]Alta-Bates Summit Medical Center, 2450 Ashby, Berkeley, CA 94705, USA
*Correspondence: eepstein@chori.org
DOI 10.1016/j.ccr.2010.11.007

SUMMARY

Basal cell carcinomas (BCCs) are hedgehog-driven tumors that resemble follicular and interfollicular epidermal basal keratinocytes and hence long have been thought to arise from these cells. However, the actual cell of origin is unknown. Using cell fate tracking of X-ray induced BCCs in Ptch1$^{+/-}$ mice, we found their essentially exclusive origin to be keratin 15-expressing stem cells of the follicular bulge. However, conditional loss of p53 not only enhanced BCC carcinogenesis from the bulge but also produced BCCs from the interfollicular epidermis, at least in part by enhancing Smo expression. This latter finding is consistent with the lack of visible tumors on ears and tail, sites lacking Smo expression, in Ptch1$^{+/-}$ mice.

INTRODUCTION

The cell of origin of most cancers has yet to be established. The majority of data thus far accumulated favor either tissue stem cells or progenitor cells of more limited regenerative capacity and differentiating plasticity as the cells that sustain the oncogenic mutation. Two strategies have been used most commonly to investigate this question. The first assesses the capacity of isolated cells to produce cancers when an activating transgene known in humans to be associated with a specific cancer type is inserted. An example is the production of leukemia-initiating cells when a leukemogenic *MLL* fusion gene is inserted into either hematopoietic stem cells or myeloid progenitor cells of a more limited differentiation spectrum (Cozzio et al., 2003). This model suggests that cells that have lost stem cell characteristics can regain that capacity when driven by an activated oncogene. The second uses cell-specific Cre expression to induce tumorigenesis, and such mapping is being used more frequently as cell-specific Cre alleles become available. Recent examples of this strategy include the use of Cre driven by the Lgr5 promoter specifically in colonic crypt stem cells to adduce evidence that these are the cells of origin of murine colon cancer (Barker et al., 2007) as well as the use of other cell-specific promoters to drive limited Cre expression (Barker et al., 2009; Le et al., 2009; Schuller et al., 2008; Wang et al., 2009; Yang et al., 2008). These recent molecular approaches complement older studies in which temporal separation of initiation and promotion of two stage skin chemical carcinogenesis argues that the cell of origin must be a stem cell since those are the only cells expected to persist for such a long duration (Morris, 2000; Perez-Losada and Balmain, 2003). We have used the second, Cre-Lox approach to investigate the identity of the cell of origin of basal cell carcinomas (BCCs) in Ptch1$^{+/-}$ mice.

BCCs, the most common human cancer, are so named because of their histologic resemblance to basal cells of the interfollicular epidermis (IFE), the hair follicle, and the sebaceous gland, i.e., the keratinocytes adjacent to the stroma. Several lines of evidence suggest that BCCs not only histologically resemble but also may arise from basal cells specifically of the hair follicles. First, BCCs express cytokeratins that more closely resemble those of follicular outer root sheath cells than those of the basal layer of the IFE, the inner root sheath, or the hair shaft (Donovan, 2009). Second, BCCs arise as the result of mutation-driven aberrant activation of Hedgehog (HH) signaling, a pathway whose activity in normal adult skin is limited essentially to follicles (Dahmane et al., 1997; Oro et al., 1997). Third, after exposure of the scalp to ionizing radiation, BCCs have occurred concomitantly with trichoblastoma (Fazaa et al., 2007), a tumor type more closely resembling the follicle. BCCs would appear to be uniquely suited for studies of the cell of cancer origin

Significance

Basal cell carcinomas, the most common of human cancers, are so named because of their resemblance to basal keratinocytes of the hair follicle, sebaceous glands, and interfollicular epidermis. However, the actual cell of origin is not known. In our ionizing radiation-treated Ptch1$^{+/-}$ mice, both cell fate mapping and enhancement of BCC carcinogenesis by deletion of p53 demonstrate conclusively that the BCCs arise from the hair follicle bulge stem cell. In mice in which basal keratinocyte p53 is deleted, BCCs can arise from the interfollicular epidermis, likely due to enhanced expression of Smo. Thus, unexpectedly, p53 may inhibit susceptibility to BCC carcinogenesis in part by affecting expression of signaling components.

because (1) activation of hedgehog signaling may be all, or at least nearly all, that is required to transform a normal keratinocyte into a BCC cell and (2) keratinocyte stem cell populations have been studied extensively and insightfully over some decades (Blanpain and Fuchs, 2009).

However, despite the indirect evidence favoring a follicular origin of BCCs, one recently published study found the murine cell of origin of cutaneous HH-driven tumors to be the IFE and not the follicle (Youssef et al., 2010). This study used cell-specific Cre to activate expression of a ROSA26-driven transgenic mutant *Smoothened* (*Smo)* whose signaling is not inhibited by *Patched 1* (*Ptch1*). By contrast, the current study was designed to address this question in a different mouse model in which HH signaling is activated by mutagenic insults of Ptch1$^{+/-}$ mice rather than by transgenic mutant *Smo*.

RESULTS

Cell Fate Mapping of Hair Follicle Bulge Cells and Their Descendents Using Yellow Fluorescent Protein in Adult Ptch1$^{+/-}$ Mice

We assessed the cell of origin of BCCs in Ptch1$^{+/-}$ mice. Normally HH signaling is inhibited by Ptch1 protein's blocking of signaling by the downstream component Smo, and this inhibition by Ptch1 is abrogated by its binding of the hedgehog ligand. *Ptch1* acts as a tumor suppressor gene; PTCH1$^{+/-}$ humans (with the basal cell nevus [Gorlin] syndrome, OMIM 109400) (Hahn et al., 1996; Johnson et al., 1996) and Ptch1$^{+/-}$ mice are highly susceptible to developing BCCs after mutagenic insults such as ionizing or ultraviolet radiation (Aszterbaum et al., 1999; Mancuso et al., 2004). Of sporadic human BCCs, approximately 90% have mutations in at least one copy of *PTCH1* while approximately 10% of sporadic BCCs carry activating mutations in *SMO* (Epstein, 2008). The most studied skin stem cell is located in the outer root sheath of the follicle, in the bulge region below the site of insertion of the arrector pili muscle (Blanpain and Fuchs, 2009; Watt and Jensen, 2009). Bulge cells are characterized by long-term self-renewal, slow cycling, and high proliferative capacity. These cells are activated periodically to enable cyclic regrowth of the hair follicle, and after wounding they can at least temporarily contribute to IFE reconstitution (Blanpain et al., 2004; Cotsarelis et al., 1990; Ito et al., 2005; Morris et al., 2004; Morris and Potten, 1999; Taylor et al., 2000; Tumbar et al., 2004). The most widely used hair follicle bulge cell markers are keratin 15 (K15), CD34, and, during telogen, Lgr5 (Cotsarelis et al., 1990; Jaks et al., 2008; Liu et al., 2003; Morris et al., 2004; Trempus et al., 2003; Tumbar et al., 2004). To determine whether these follicular bulge stem cells might be the cell of origin of murine BCCs, we produced Ptch1$^{+/-}$ mice in which RU-486-regulated Cre is expressed under the control of a bulge-specific promoter: K15-CrePR1 (Morris et al., 2004). For fate mapping, we crossed these Ptch1$^{+/-}$ K15CrePR1 mice with ROSA26 reporter mice that express enhanced yellow fluorescent protein (YFP) following Cre-mediated excision of a loxP-flanked transcriptional stop sequence (lsl) (Srinivas et al., 2001). We treated the resulting Ptch1$^{+/-}$ K15CrePR1 YFP lsl/lsl mice, designated "Y15," with RU-486 for 3 days at age 7.5 weeks, an age when hair follicles are in telogen and K15 expression is restricted to the follicle bulge region (Morris et al., 2004) (Figure 1A). Thus, in these mice, K15-expressing bulge stem cells and their descendants express YFP. For comparison, we activated Cre in Ptch1$^{+/-}$ mice in which its expression is driven by the K14 promoter, i.e., Ptch1$^{+/-}$ K14-CreER2 YFP lsl/lsl ("Y14") mice, by 3 days of treatment with tamoxifen at age 7.5 weeks. The K14 promoter is transcriptionally active in the basal cells of the follicle, the IFE, and the sebaceous glands. To confirm the RU-486- or tamoxifen-dependent tissue specific activation of YFP expression, we biopsied skin of Y15 or Y14 mice 1 day after the last dose of RU-486 or tamoxifen treatment and assessed the location of YFP expression. As shown in Figure 1, RU-486-treated Y15 mice expressed YFP in the follicle bulge region, colocalizing with K15 expression (Figures 1B and 1C). The IFE essentially lacked YFP expression. By contrast, tamoxifen-treated Y14 mice expressed YFP in epidermal basal cells, irrespective of K15 expression (Figures 1D and 1E). We noted that not all K15-expressing bulge cells expressed YFP in Y15 mice. By contrast tamoxifen-treated Y14 mice had only occasional unlabeled follicles or IFE basal cells. To compare the efficiency of YFP activation driven by the two Cre alleles, we quantitated YFP labeling of K15-expressing cells in skin biopsies of Y15 and Y14 mice (five mice per group). In Y15 mice, approximately 56% (ranging from 36% to 69%) of K15-expressing cells also expressed YFP. In Y14 mice, approximately 83% (ranging from 62% to 94%) of K15-expressing cells expressed YFP. This lack of 100% labeling efficiency is consistent with findings of others (Liu et al., 2003; Srinivas et al., 2001). The greater percentage of YFP-labeled K15-expressing cells in the K14-CreER2 mice indicates a more efficient expression and/or activation of the CreER2/tamoxifen than of the CrePR1/RU-486 system in K15-expressing follicular cells.

YFP-Expressing Microscopic and Macroscopic BCCs Arise in Y15 and Y14 Mice

One day after the last dose of RU-486 or tamoxifen (age 8 weeks), when YFP-positive cells in Y15 mice remained confined to the bulge, we treated the mice with 4Gy of ionizing radiation. At age 9 months, grossly normal appearing dorsal skin of both Y15 and Y14 mice contained YFP-positive and YFP-negative microscopic BCCs (Figures 2A and 2B). The fraction of tumors that were YFP-positive was consistent with the percentage of the K15-expressing follicle cells that were YFP+ (49% versus 56% for Y15 and 77% versus 83% for Y14). Although tumors appeared in random sections to be in close proximity to either the follicle or to the IFE, careful examination of serial sections of skin biopsies indicated that more than 90% of microscopic BCCs in Y14 or Y15 mice had direct connections with a follicle in at least one section (Figures 2C to 2F). The few remaining tumors may indeed have arisen from IFE cells, or their apparent lack of connection to the follicle may have been an artifact due, e.g., to missed sections. In addition, we found no significant differences in the tumor burden (tumor multiplicity and sizes of the microscopic tumors) between YFP-expressing mice and non-YFP-expressing control mice (Ptch1$^{+/-}$ YFP lsl/lsl littermates lacking Cre), indicating that the expression of YFP did not affect skin keratinocyte BCC tumorigenesis.

Starting at age 9 months, consistent with our past experience with Ptch1$^{+/-}$ mice, some mice developed macroscopic BCCs. We found strong YFP staining in tumor cells and no such staining

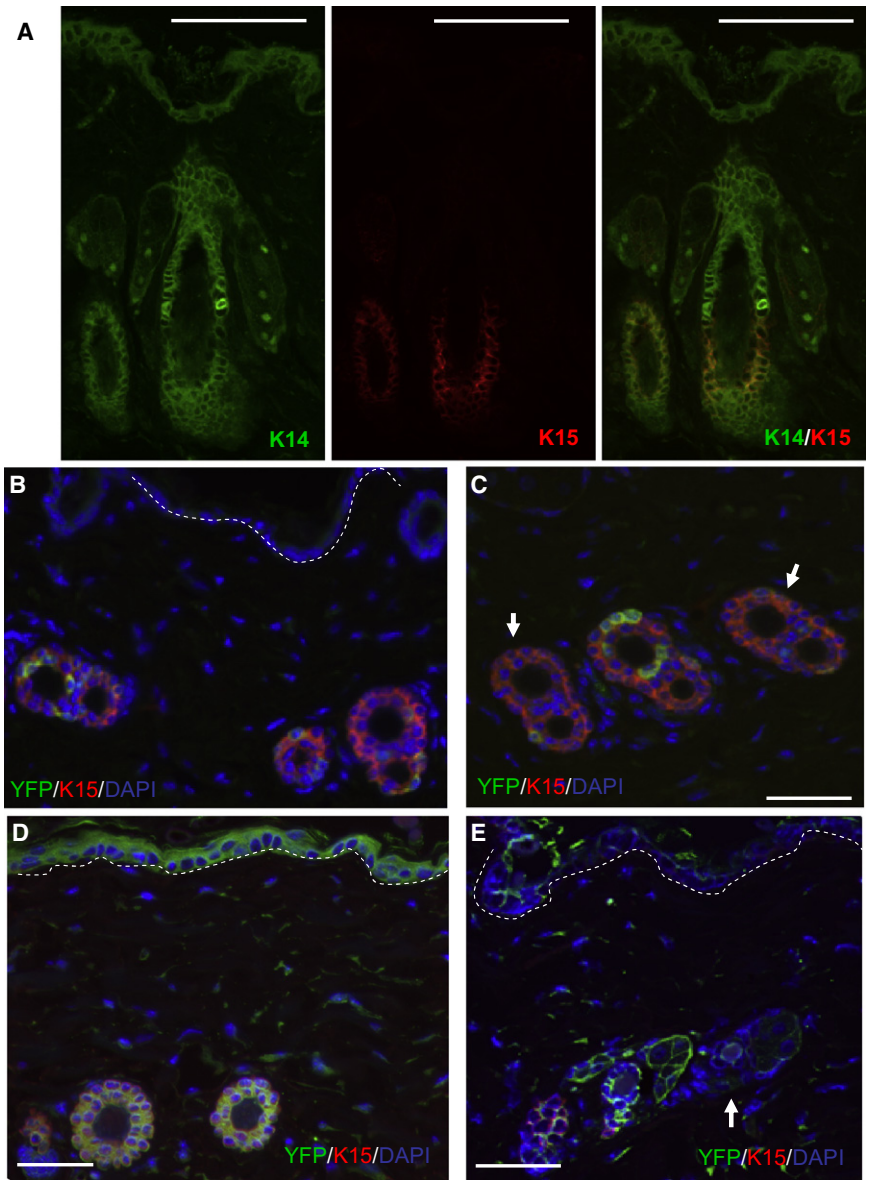

Figure 1. K15- or K14-Expressing Cells Are Specifically Marked with YFP in Adult Y15 or Y14 Mice

One day after the last dose of RU-486 or tamoxifen, the skin of Y15 or Y14 mice were biopsied and immunostained with anti-K15, anti-K14 or anti-YFP antibodies. Color coding indicates antibody labeling. Scale bars = 50 μm.

(A) A selective image shows that K15-expressing cells are restricted to the bulge region and the K14-positive cells line the whole hair follicle including the isthmus region, as well as the IFE.

(B) In Y15 mice, YFP was present in K15-expressing follicles but absent from IFE (dashed line).

(C) In Y15 mice, some K15-expressing follicles failed to express YFP (arrows).

(D) In Y14 mice, YFP was present in both follicles and in the IFE.

(E) In Y14 mice, occasional regions of IFE or follicles (arrows) were free of YFP expression.

in stromal regions in both Y15 and Y14 mice (Figure 3A). Consistent with our findings 1 day after Cre activation, YFP expression in normal appearing skin surrounding BCCs in Y15 mice was limited to follicles (Figure 3B) but was present in both the IFE and follicles in Y14 mice. YFP-negative visible tumors, like YFP negative microscopic BCCs at age 9 months, were present in both Y15 and Y14 mice. These might have arisen from non-K15 expressing cells and/or from K15-expressing cells in which RU486-mediated Cre activation failed to delete the lsl sequence. Because only a small number of macroscopic tumors developed, our study had insufficient statistical power to assess the correlation between the percentage of visible YFP-expressing tumors and the YFP-labeling efficiency of hair follicles.

Taken together, these cell fate mapping studies indicate that K15-expressing cells are the predominant, and likely the exclusive, cells of origin of BCCs in ionizing radiation-treated Ptch1$^{+/-}$ mice.

BCC Tumorigenesis in Ptch1$^{+/-}$ p53$^{-/-}$ Mice

Ptch1$^{+/-}$p53$^{-/-}$ mice develop early and near uniformly fatal medulloblastomas (Wetmore et al., 2001). Similarly, we have observed dramatic acceleration of BCC formation in Ptch1+/− mice in which p53 deletion is limited to K14-expressing keratinocytes (G.Y.W., E.H.E., unpublished data). Hence as a second indicator of the cell of origin of BCCs, we compared the enhancement of BCC carcinogenesis when we deleted p53 in the follicular bulge subset of basal keratinocytes with the enhancement when we deleted p53 in all basal keratinocytes - Ptch1$^{+/-}$ K15CrePR1 p53$^{fl/fl}$ (“PF15”) and Ptch1$^{+/-}$ K14CreER2 p53$^{fl/fl}$ (“PF14”) mice. Since p53 functions primarily in a cell autonomous manner, we expected that deletion of p53 in K15-expressing cells would also enhance BCC carcinogenesis were K15-expressing cells indeed the BCC cell of origin.

We activated Cre endonuclease and treated with ionizing radiation as in the Y14 and Y15 mouse studies, i.e., RU-486 or tamoxifen injection at age 7.5 weeks for 3 days followed the next day by ionizing radiation. Control Ptch1$^{+/-}$ p53$^{fl/fl}$ (lacking a Cre transgene) mice generated either from PF15 or PF14 breedings had similar microscopic tumor burden, confirming that mice of the two genotypes shared a similar baseline level of tumor susceptibility.

Both PF15 and PF14 mice developed macroscopic BCCs from age 5 to 8 months, an age significantly younger than the age 9–13 months when p53 wild-type Y15 and Y14 mice developed visible BCCs (Kaplan-Meyer curve, $p < 0.01$, Figure 4A). Despite the same tumor latency and tumor incidence (100% macroscopic tumor-bearing mice in both PF15 and PF14 genotypes), PF14 mice had considerably greater tumor multiplicity

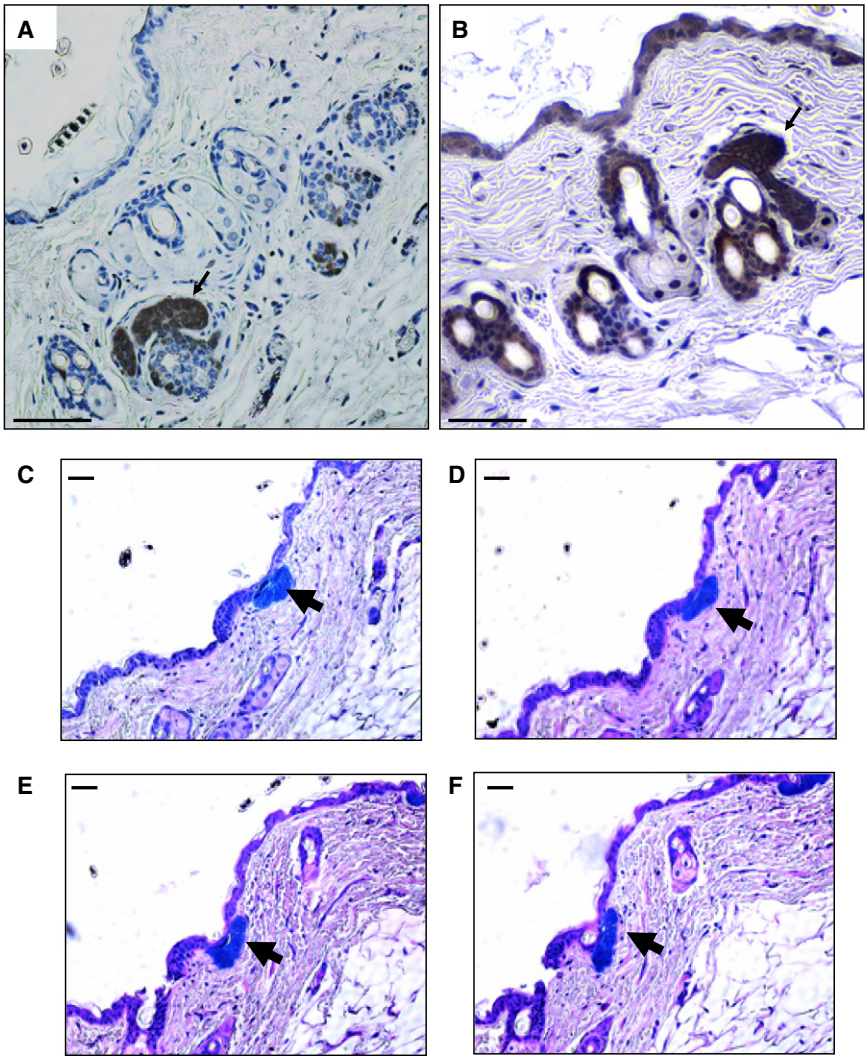

Figure 2. YFP-Expressing Microscopic BCCs Arise from Y15 and Y14 Mice

(A and B) The skin biopsies of Y15 (A) and Y14 (B) mice were immunostained with anti-YFP antibody (brown) and counterstained with hematoxylin (blue). Arrows denote the representative YFP-positive microscopic BCCs. Scale bars = 50 μm. (C to F) Representative images of serial sections of a skin biopsy. A total of 15 serial sections of 5 μm in thickness per section were stained with H & E and examined for any hair follicle connection of every single microscopic BCC on all serial sections. Selective images represent sections from one sample that show no connection to the follicle in (C) and (D) and surrounds a follicle in (E) and (F). Arrows indicate microscopic BCC. Scale bars = 50 μm.

(average number of tumors per mouse) than did PF15 mice, in particular at age 7 and 8 months (Fold = 5, $p < 0.01$) (Figure 4B).

Consistent with the differing numbers of visible BCCs, we found 70% more microscopic BCCs at age 5 months in PF14 mice than in PF15 mice ($p < 0.01$). Interestingly, the fraction of microscopic BCCs that were free of follicle connection, i.e., IFE-microscopic BCCs, on serial sections was significantly increased in PF14 mice over that in PF15 (TTEST, $p < 0.05$) or (p53-wild-type) Y15 or Y14 mice ($p < 0.01$, Figure 5). The significant enhancement of IFE-microscopic BCCs in PF14 mice compared to PF15, Y15, and Y14 mice suggests that loss of p53 sensitizes IFE cells to BCC tumorigenesis.

Two Different BCC Subtypes

Next, we classified the macroscopic BCCs in the four groups of mice into two histopathologic subtypes (Figure 6). Type I BCCs had branching and radiating tumor cells, more reminiscent of follicular differentiation, and some cells contained smooth muscle actin (SMA). Type II BCCs had basaloid cells arrayed in nests not resembling follicular differentiation and lacked tumor cell SMA staining. Additionally, type I tumors had more extensive stroma than did type II tumors. Tumors in PF15, Y15, and Y14 mice were 95%–100% of type I (Figure 5). However, in PF14 mice, only 80% of the tumors were of type I; the remaining 20% were of type II. Thus, PF14 mice have both more microscopic BCCs lacking connection to the follicle and more visible BCCs of type II histology. The correlation (nonparametric correlation, Spearman, $p = 0.04$) suggests that murine BCCs arising from the IFE are more likely of type II histology, consistent with the finding of Mancuso and colleagues that SMA-expressing BCCs arise from follicles (Mancuso et al., 2006).

SMO Is Necessary for BCC Tumorigenesis

In general, mouse models in which the HH pathway is activated downstream of Ptch1, e.g., transgenic expression of SmoM2 and Gli2, produce HH-driven tumors predominantly on the ears and tail. By contrast, no visible BCCs and only occasional basaloid hyperproliferation and (at ages later than on dorsal skin) microscopic BCCs develop at these sites in our Ptch1$^{+/-}$ mice. To investigate one possible basis for the differing sites of BCC development in the different models, we used immunostaining to analyze tissue distribution of Smo protein expression. The great majority of follicles of the ear and tail of Ptch1$^{+/-}$ mice fail to express immunohistochemically detectable Smo protein (Figures 7A–7C). An exception to this is the elongated anagen follicle which, like follicles of similar morphology in the dorsal skin, does express Smo. But we found such follicles only rarely in tail and not at all in ear tissue. In dorsal skin of Ptch1$^{+/-}$, p53 wild-type (i.e., Y14 and Y15, Figures 7D and 7E) mice, Smo staining occurs in hair follicles (anagen) and in some, albeit not all, microscopic tumors. Dorsal skin IFE expresses essentially no immunohistochemically detectable Smo protein. Upon K14-Cre mediated deletion of *p53*, we found increased Smo expression not only in the follicles but also, crucially, in the IFE (Figures 7F and 7G). These data suggest that Ptch1$^{+/-}$, p53 wild-type mice fail to develop

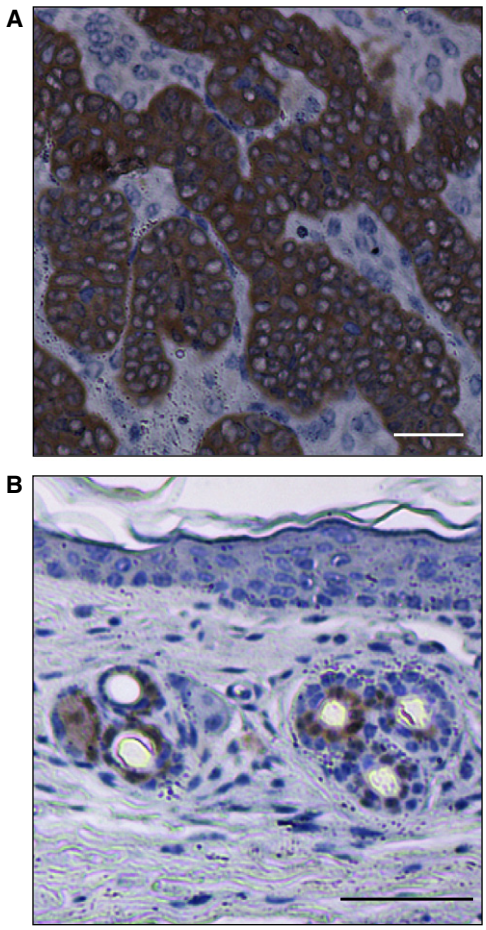

Figure 3. YFP-Expressing Macroscopic BCC Tumors Arise from Y15 Mice

(A) A representative macroscopic BCC generated from Y15 mice was stained with anti-YFP antibody (brown) and counterstained with hematoxylin (blue). Scale bar = 50 μm.

(B) Examination of the normal-looking skin surrounding the tumor confirmed that follicles expressed YFP while the IFE was free of YFP expression. Scale bar = 50 μm.

BCCs on the ears, tails, and dorsal IFE because they do not express significant amounts of Smo protein at these sites, and therefore loss of Ptch1 is irrelevant to HH activation. Correspondingly, increased expression of Smo in the IFE in mice in which *p53* has been deleted from the IFE correlates with development of microscopic BCCs at these sites.

An additional discrepancy between SmoM2 mice (Yousseff et al., 2010) and our Ptch1$^{+/-}$ mice is the failure of the former to generate tumors in the follicle, despite follicular expression of the transgene (Yousseff et al., 2010) and the arising of tumors exclusively from the follicle in the latter. One possible explanation for this difference is that Ptch1 protein might have functions other than the inhibition of HH signaling. One described such non-HH function of Ptch1 is the tethering of cyclin B1 in the cytoplasm and consequent prevention of its normal function in the nucleus (Barnes et al., 2001). Therefore, we compared the location of cyclin B1 in tumors arising in the two models. As predicted, cyclin B1 is predominantly cytoplasmic in

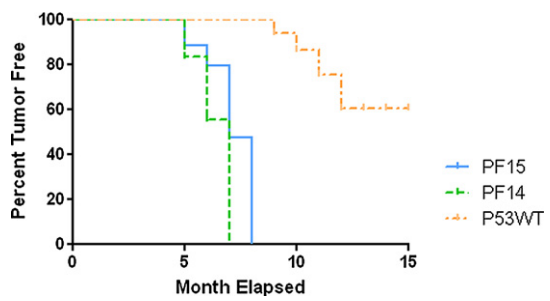

B

	PF15	PF14	Fold	*p* value
Microscopic BCCs				
5 mon	26.33 ± 10.17	47.86 ± 6.16.30	1.69	0.01
Macroscopic BCCs				
5 mon	0.25 ± 0.46	0.63 ± 0.92	2.00	0.48
6 mon	0.63 ± 0.74	2.88 ± 2.64	3.97	0.06
7 mon	1.86 ± 1.57	7.86 ± 3.60	4.80	0.01
8 mon	2.50 ± 1.05	12.20 ± 2.17	4.90	0.01

Figure 4. Deletion of p53 Specifically in Either K15- or K14-Expressing Cells Accelerates BCC Tumorigenesis in Ptch1$^{+/-}$ Mice

(A) Tumor latency of macroscopic BCC development in PF15, PF14, and p53WT (combined data of Y15 and Y14) were analyzed with Kaplan-Meier curve ($p < 0.01$).

(B) The tumor multiplicity of microscopic and macroscopic BCC was assessed at mouse age 5–8 months. Fold differences between PF14 and PF15 mice and p values are shown. Data are shown as means ± SD (n = 8).

HH-driven tumors of SmoM2 mice whereas in marked contrast it is clearly nuclear in BCCs of IR-treated Ptch1$^{+/-}$ mice (Figure 8). This difference suggests that BCCs arising from the follicle may require nuclear cyclin B1, whereas tumors arising from the IFE may not require cyclin B1 nuclear action.

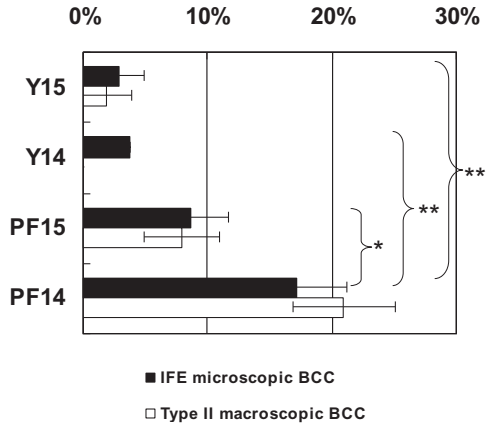

Figure 5. The Ratio of IFE Microscopic BCCs Is Increased in PF14 Mice and Appears Associated with Type I Macroscopic BCCs

The fraction of microscopic BCCs that were free of follicle connection, i.e., the IFE microscopic BCCs, is plotted with the percentage of type II macroscopic tumors. Data are normalized against total number of tumors and shown as mean ± SD (n = 4) with p values < 0.05 (*) or < 0.01 (**).

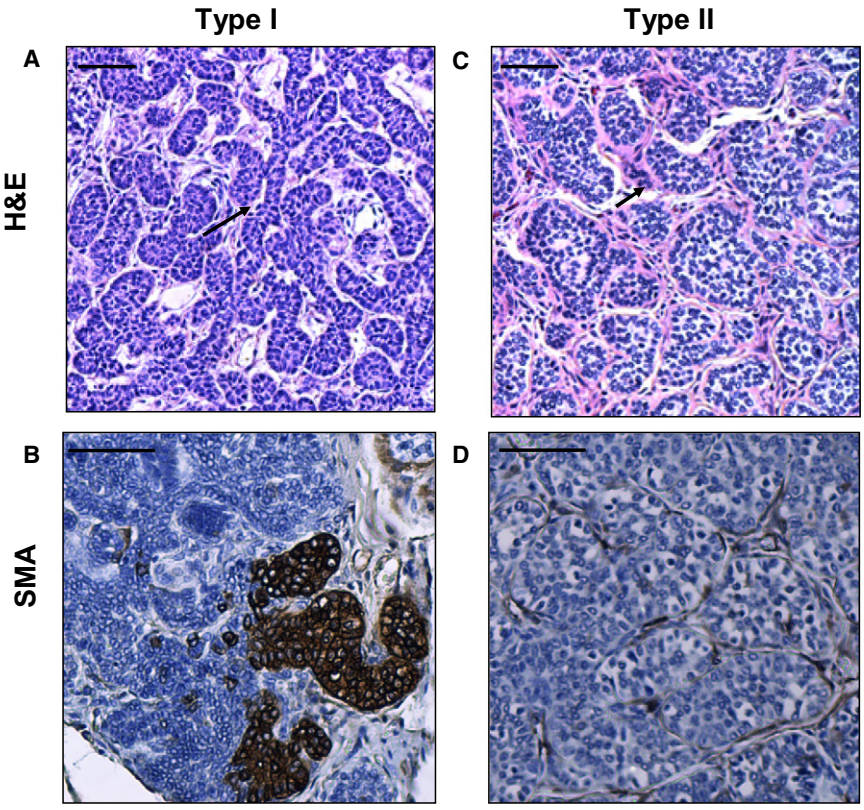

Figure 6. Two Distinct Histopathologic Subtypes of Macroscopic BCCs

(A and B) Representative images of type I histologic feature show branching, radiating tumor structure (arrow) and patchy expression of SMA (brown) in tumor cells. Scale bar = 50 μm.

(C and D) Representative images of type II histologic feature show nests of tumor cells and positive SMA staining limited to the stroma. Scale bar = 50 μm.

DISCUSSION

These studies generate several conclusions. The first is that IR-induced BCCs in Ptch1$^{+/-}$ mice arise predominantly, and likely exclusively, from K15 expressing hair follicle bulge stem cells. Thus, activation of YFP expression in K15-expressing adult mouse follicle bulge stem cells produces YFP-positive microscopic and macroscopic BCCs, and deletion of p53 limited to these same cells dramatically enhances BCC tumorigenesis. We believe that the most parsimonious explanation for the presence of non-YFP expressing BCCs is the variable, less than 100% efficiency of Cre-mediated activation of YFP expression because in the Y14 and Y15 mice the fraction of BCCs that are YFP+ is similar to the fraction of K15+ follicular cells that are YFP+ and because we find a direct physical connection between follicle and microscopic BCCs in nearly all IR-treated wild-type p53, Ptch1$^{+/-}$ mice. However, we cannot exclude completely the possibility that a small fraction of YFP nonexpressing BCCs in these mice might have arisen from cells of the IFE. On the other hand, we and others (Liu et al., 2003) observe occasional, randomly distributed K15-expressing cells in the adult IFE, suggesting the possibility that some YFP-positive BCCs could originate from these K15-expressing IFE cells. Since there is no marker available for the specific targeting of keratinocytes that express K14 but not K15, it is not possible to address this question directly.

By contrast, our data indicate that the higher numbers of BCCs in mice in which p53 is deleted not only from the follicular bulge but also from the IFE are due at least in part to a contribution by non-K15-expressing cells to tumor formation, since in PF14 mice we find significant numbers of microscopic BCCs with no detectable physical connection to the follicle. In addition, some of the visible BCCs that these PF14 mice develop have a histologic pattern that differs from the pattern of BCCs arising from the follicles. Our correlation of the tumor phenotype of SMA expression with follicular origin is highly congruent with data obtained by Saran's group using a different Ptch1$^{+/-}$ model (Mancuso et al., 2006). As they noted, several authors have identified human BCCs expressing SMA but contrary to expectations the degree of aggressiveness of human BCCs has been reported most recently to correlate with SMA expression in the stroma, not in the tumor cells (Adegboyega et al., 2010).

Second, our results highlight phenotypic differences between HH-driven cutaneous tumorigenesis in Ptch1$^{+/-}$ mice versus in other murine models. One such difference is the body location of tumor formation. Thus, in models in which tumorigenesis is driven by abnormal alleles of downstream HH signaling genes, activating mutations of Smo, heterozygosity for SuFu (Svard et al., 2006), or overexpressed Gli2 (Hutchin et al., 2005) (albeit not overexpressed Gli1; Nilsson et al., 2000) macroscopic tumors that arise are located predominantly on the ears, tails, and paws, whereas we have never seen a visible BCCs at these sites in a decade of studies of Ptch1$^{+/-}$ mice. Our finding that Smo is not expressed in the skin at these sites offers an attractive explanation for this discrepancy. In so far as the function of Ptch1 is to inhibit Smo signaling, its loss in cells not expressing Smo should be of little consequence—activation of HH signaling by loss of Ptch1 function by ligand-binding (Walter et al., 2010) or by inactivating mutation requires expression of downstream components of the signaling machinery. Similarly, we believe the discrepancy between our findings of a follicular origin of BCCs and Yousseff et al.'s finding of an IFE origin of HH-driven tumors arises at least in part because they used a mutant Smo allele driven by a ROSA-26 promoter, thus bypassing low Smo expression in the IFE of p53 wild-type mice. Hence, the induction of Smo IFE expression correlates with the lack or presence of BCC tumorigenesis of this region.

There is an additional discrepancy between conclusions reached with the two models; mice with activated Smo

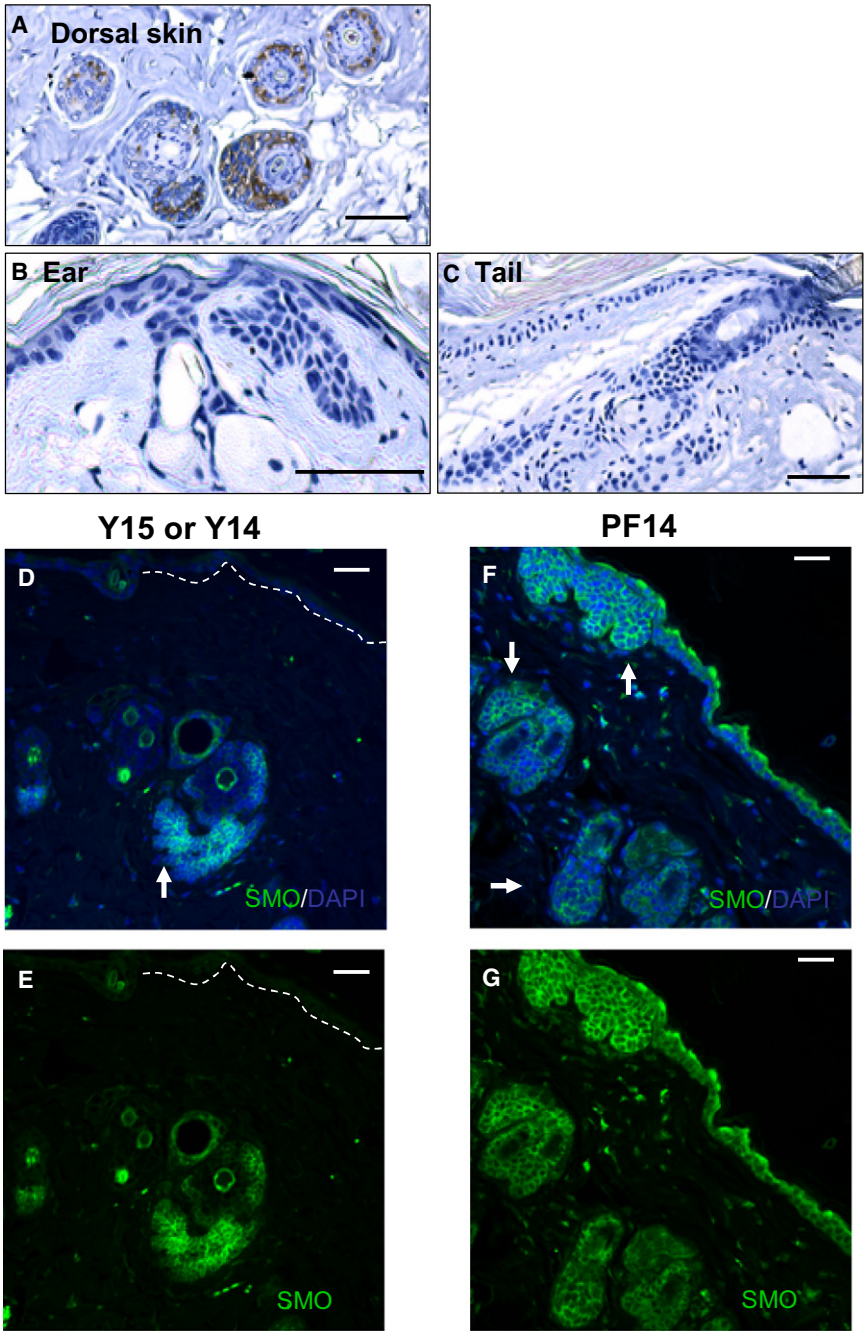

Figure 7. Differential Expression of Smo

(A–C) Representative images of immunostaining with anti-Smo antibody (brown) and counterstained with hematoxylin (blue) show absence of staining in ear or tail and positive staining in dorsal skin follicles.

(D and E) The skin biopsy of Y14 or Y15 mouse that is immunostained with anti-Smo antibody (green) shows that Smo is detected in follicles and some microscopic BCCs (arrows) but not in IFE (dashed line). (E) No DAPI counter staining. Scale bars = 50 μm.

(F and G) The skin biopsy of PF14 mouse that is immunostained with anti-Smo antibody (green) shows that Smo is detected in follicles and some microscopic BCCs (arrows) as well as in IFE (dashed line). (G) No DAPI counter staining. Scale bars = 50 μm.

developed follicular hyperplasia but no follicular BCCs (Youssef et al., 2010), suggesting that follicular bulge cells are resistant to transformation by hedgehog signaling (Ridky and Khavari, 2010). One potential explanation for this discrepancy is that tumorigenic transformation of K15+ cells might require loss of functions of Ptch1 other than its inhibition of HH signaling. Indeed Ptch1 protein has been described as inhibiting cell cycle progression via tethering cyclin B1 in the cytoplasm and preventing its access to the nucleus (Barnes et al., 2001), and our finding of differential localization of cyclin B1 in the two models is consistent with that hypothesis. Other currently cryptic non-HH functions of Ptch1 may exist. A relative requirement for ablation of non-HH inhibitory function(s) of Ptch1 might be one reason that the great majority of human BCCs carry mutations of Ptch1 rather than of other components of the HH pathway despite the ability of engineered mutants of downstream components to drive murine BCC tumorigenesis.

Third, our finding that deletion of p53 increases expression of keratinocyte Smo is of particular interest in that human BCCs, which frequently carry mutant p53 (Ling et al., 2001; Reifenberger et al., 2005), typically arise on chronically sun damaged skin containing clones of epidermal keratinocytes expressing mutant p53 (Backvall et al., 2004; Ziegler et al., 1994). Thus such p53 mutations may render human IFE cells competent for the development of BCCs, in part by enhancing expression of SMO protein. This suggests that the p53 mutations in human BCCs are not simply passengers due to the arising of BCCs on skin containing mutant p53 but rather are direct contributors to BCC carcinogenesis, in part by enhancing expression of SMO and thereby sensitizing epidermal keratinocytes to the oncogenic effects of PTCH1 loss. Furthermore, they would provide an explanation for the seeming conundrum that some mutations in PTCH1 and p53 in human BCCs are of the UVB signature type (Aszterbaum et al., 1998; Chidambaram et al., 1996; Gailani et al., 1996a, 1996b; Lench et al., 1997; Rady et al., 1992; Unden et al., 1996; Wicking et al., 1997; Wolter et al., 1997) even though human hair follicle bulge stem cells may be too deep in the dermis to be reached by mutagenic UVB. Of interest, p53 loss can enhance normal neural stem cell self-renewal (Meletis et al., 2006), rescue epidermal stem cell function in telomerase-deficient mice (Flores and Blasco,

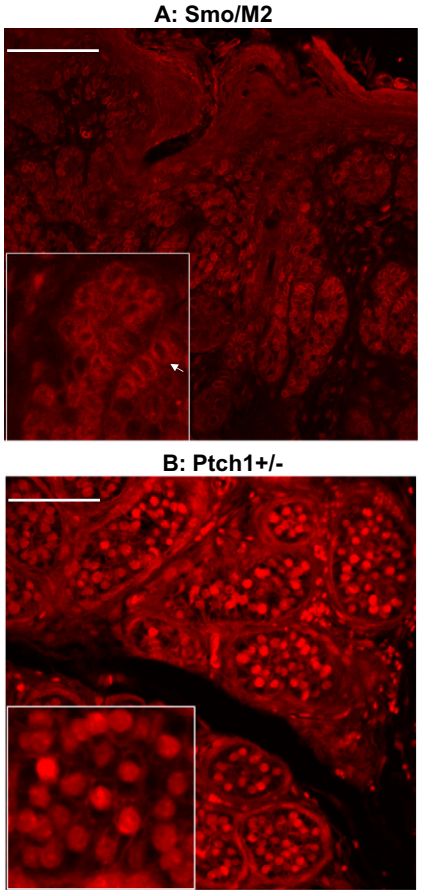

Figure 8. Differential Localization of Cyclin B1 in BCCs Developed from Ptch1$^{+/-}$ or Smo/M2 Mouse Model

Representative immunostained images with anti-cyclin B1 antibody (red). Insets are images in higher magnification. Scale bars = 50 μm.

(A) Cutaneous tumor of Smo/M2 mouse shows cells with generally weak and cytoplasmic cyclin B1 (arrows).

(B) BCC of Ptch1$^{+/-}$ mouse has cells with strong nuclear cyclin B1.

2009), and enhance reprogramming of somatic cells, in particular human keratinocytes, to a more stem-like state (Kawamura et al., 2009), and hedgehog signaling may be important for maintenance of normal tissue and cancer stem cells (Agarwal and Matsui, 2010; Scales and de Sauvage, 2009; Zhao et al., 2009). Thus increased expression of Smo may be one mechanism by which p53 loss contributes to stemness. Furthermore, there is a parallel between newer views of p53's role in influencing cell size and the finding that Ptch1$^{+/-}$ humans and mice are larger than their Ptch1 wild-type siblings (Goodrich et al., 1997; Milenkovic et al., 1999); perhaps inhibition of HH signaling by p53 via Smo downregulation might be another mechanism underlying this inhibition of cell growth by p53 (Gottlieb and Vousden, 2010; Vousden and Ryan, 2009).

The possibility that stem cells of the follicle are the cells of origin of cutaneous cancers is one that has been considered since, and even before, the initial localization of such cells to the bulge (Cotsarelis et al., 1990). The current view is that these cells can serve as the reservoir that regenerates the active, hair-producing lower portion of the follicle that functions for a limited time (anagen) before entering regressing (catagen) and then resting (telogen) phases (Blanpain and Fuchs, 2009). These cells also can repopulate the IFE, not under normal homeostasis but only following injury and likely only transiently (Claudinot et al., 2005; Ghazizadeh and Taichman, 2001; Ito et al., 2005; Langton et al., 2008; Levy et al., 2005). Recently, the hair germ that lies at the lower end of the bulge has been identified as the proximate source of the lower follicle and can be identified specifically by expression of Lgr5, which also is a marker of stem cells in the colon (Barker et al., 2007; Jaks et al., 2008; Sato et al., 2009). In addition, Lgr6-expressing cells located above the bulge appear to be one postnatal stem cell population of the IFE and sebaceous glands (Snippert et al., 2010). These cells express K14 but not K15 (Snippert et al., 2010; Figure 1A), and hence despite their postulated role as the most primitive of epidermal stem cells, are not the cell of origin of BCCs in p53 wild-type mice. Thus, it is possible that susceptibility to transformation to BCCs by HH activation requires some commitment to a more differerentiated fate. Of note, HH-induced murine medulloblastomas occur only when precursors have committed to granule cell lineage, irrespective of whether or not the mutation is present in earlier stage stem cells (Schuller et al., 2008; Yang et al., 2008).

In summary, based both on fate mapping and on the impact of p53 deficiency on BCC tumorigenesis, we conclude that K15-expressing cells are the predominant cells of origin of Ptch1$^{+/-}$ murine BCCs, irrespective of p53 status. The loss of p53 significantly enhances the tumor-initiating capacity not only of follicular cells but also of non-K15 expressing cells, such as those of the IFE. Furthermore, comparison of HH-driven carcinogenesis in Ptch1$^{+/-}$ mice versus in Smo-Mut mice points to the essential role of expression of Smo in BCC carcinogenesis and suggests a functional role for the cytoplasmic tethering of cyclin B1 by Ptch1 protein.

EXPERIMENTAL PROCEDURES

Generation of Transgenic Mice and IR-Induced BCC Tumorigenesis

Mice carrying engineered alleles were kindly provided by A. Berns (p53$^{fl/fl}$) (Jonkers et al., 2001), P. Chambon, (K14-Cre-ER2) (Indra et al., 2000), F. Costantini (ROSA26 YFP lsl) (Srinivas et al., 2001), and G. Cotsarelis (K15-Cre-PR1)(Morris et al., 2004). For lineage analysis, K15-CrePR1 and K14-CreER2 mice were crossed with ROSA26 floxed-stop YFP and Ptch1$^{+/-}$ mice (Aszterbaum et al., 1999) to generate Ptch1$^{+/-}$ K15-Cre-PR1 YFP lsl/lsl (Y15 mice) or Ptch1$^{+/-}$ K14-Cre-ER2 YFP lsl/lsl (Y14 mice). For p53 deletion studies, K15-CrePR1 and K14-CreER2 mice were crossed with p53$^{fl/fl}$ and Ptch1$^{+/-}$ mice to generate Ptch1$^{+/-}$ K15-Cre-PR1 p53$^{fl/fl}$ (PF15 mice) or Ptch1$^{+/-}$ K14-Cre-ER2 p53$^{fl/fl}$ (PF14 mice). To minimize any genetic background differences in susceptibility to BCC formation, we intercrossed PF15 and PF14 mice to produce offspring of similar backgrounds. All mice were genotyped by PCR amplification of genomic DNA extracted from tail snips using DirectPCR Lysis Reagent (Tail) following the manufacturer's instruction (Viagen Biotech, Los Angeles, CA). The primer sequences and PCR conditions were described previously (Indra et al., 2000; Jonkers et al., 2001; Morris et al., 2004; Srinivas et al., 2001). Mice were housed under standard conditions (fluorescent lighting 12 hr per day, room temperature 23°C–25°C, and relative humidity 45%–55%). Animal care and use were in compliance with the protocols approved by the Institutional Animal Care and Use Committee (IACUC) of Children's Hospital Oakland Research Institute (CHORI).

To activate Cre-mediated recombinase activity, mice were injected intraperitoneally with 750 μg RU486 (Y15 and PF15) or 100 μg tamoxifen (Y14 and

PF14, Sigma-Aldrich, St Louis, MO) daily at age 7.5 weeks for 3 consecutive days. On the day following the last dose of treatment (i.e., age 8 weeks), mice were subjected to IR at 4 Gy, 160 kV using an X-ray source (RadSource RS2000 irradiator). The few Ptch1$^{+/-}$ K15-CrePR1 YFP lsl/lsl mice with significant numbers of YFP+ IFE cells in the 9 month biopsies were removed from further analyses.

Skin Sampling and β-Galactosidase Staining

Standard mouse dorsal skin biopsy and β-galactosidase staining were performed as described previously (Aszterbaum et al., 1999) except that a 1 × 1.5 cm rectangular area of skin was excised and divided into five slivers of 1 cm in width. After fixation with 2% formaldehyde (Fisher Scientific) 0.2% glutaraldehyde mixture (Sigma), tissues were stained with a β-Gal Staining Set according to the manufacturer's instruction (Roche Diagnostics, Penzberg, Germany) followed by standard paraffin embedding, sectioning, and hemotoxylin and eosin (H&E) stain. The stained slides were scanned into digital images by Aperio (Vista, CA), which were used to examine microscopic tumor multiplicity using Aperio ImageScope software (v9.1.19.1569).

Immunostaining

Paraffin sections were deparaffinized and rehydrated. For immunohistochemistry, rehydrated samples were subjected to antigen retrieval with rodent decloaker (Biocare Medical, Concord, CA) for 10 min at 95°C –100°C, followed by incubation with rodent block M (Biocare Medical) for 15 min, primary antibody for 1 hr, and secondary antibody, rabbit on rodent HRP-polymer or MM HRP-polymer for 20 min (Biocare Medical). Signal was developed using liquid DAB+ substrate (Dako, Carpinteria, CA) for 2-10 min and counterstained with Cat hematoxylin (Biocare Medical) or Methyl green (Trevigen). The primary antibodies were rabbit anti-YFP (1: 3000, Abcam, Cambridge, MA), rabbit anti-Smo (1:200, Abcam), or mouse anti-SMA (1: 500, Sigma). For immunofluorescent staining, antigen retrieved slides were blocked with 2% FBS followed by incubation with primary antibodies: rabbit anti-YFP (1:100), anti-Smo (1:100, LS-A2668, MBL, Woburn, MA) or mouse anti-cyclin B1 (1: 200, Invitrogen, Camerillo, CA) overnight at 4°C. The secondary antibody conjugated with Alexa Fluor 488 or 555 (1:1000, Molecular Probes, Eugene, OR) was used together with DAPI (1:5000, Molecular Probes) to detect primary antibodies followed by mounting with ProLong Gold Antifade Reagents (Molecular Probes). All images were acquired using Nikon Eclipse E600 microscopy and processed with imaging software IPLab (Scanalytics).

Statistical Analysis

All values are shown as mean ± standard deviation (SD). Nonparametric t test (Mann-Whitney test), nonparametric correlation (Spearman), and Kaplan Meier survival curve were performed to determine the statistical significance (GraphPad Prism 4.0).

ACKNOWLEDGMENTS

We thank those who contributed mice containing mutant alleles as listed in the Experimental Procedures; Sam Test for invaluable assistance with microscopy; Anj Dlugosz and Marina Grachtchouk for tumors blocks from mutSmo mice (Grachtchouk et al., 2003) and for extremely helpful suggestions; M Bosenberg for helpful suggestions; and Eileen Cheryl Libove, Yefim Khaimskiy, Lynn Wang, and other members of our lab for invaluable assistance.

Received: June 25, 2010
Revised: September 8, 2010
Accepted: November 3, 2010
Published online: January 6, 2011

REFERENCES

Adegboyega, P.A., Rodriguez, S., and McLarty, J. (2010). Stromal expression of actin is a marker of aggressiveness in basal cell carcinoma. Hum. Pathol. *41*, 1128–1137.

Agarwal, J.R., and Matsui, W. (2010). Multiple myeloma: a paradigm for translation of the cancer stem cell hypothesis. Anticancer. Agents Med. Chem. *10*, 116–120.

Aszterbaum, M., Rothman, A., Johnson, R.L., Fisher, M., Xie, J., Bonifas, J.M., Zhang, X., Scott, M.P., and Epstein, E.H., Jr. (1998). Identification of mutations in the human PATCHED gene in sporadic basal cell carcinomas and in patients with the basal cell nevus syndrome. J. Invest. Dermatol. *110*, 885–888.

Aszterbaum, M., Epstein, J., Oro, A., Douglas, V., LeBoit, P.E., Scott, M.P., and Epstein, E.H., Jr. (1999). Ultraviolet and ionizing radiation enhance the growth of BCCs and trichoblastomas in patched heterozygous knockout mice. Nat. Med. *5*, 1285–1291.

Backvall, H., Stromberg, S., Gustafsson, A., Asplund, A., Sivertsson, A., Lundeberg, J., and Ponten, F. (2004). Mutation spectra of epidermal p53 clones adjacent to basal cell carcinoma and squamous cell carcinoma. Exp. Dermatol. *13*, 643–650.

Barker, N., van Es, J.H., Kuipers, J., Kujala, P., van den Born, M., Cozijnsen, M., Haegebarth, A., Korving, J., Begthel, H., Peters, P.J., and Clevers, H. (2007). Identification of stem cells in small intestine and colon by marker gene Lgr5. Nature *449*, 1003–1007.

Barker, N., Ridgway, R.A., van Es, J.H., van de Wetering, M., Begthel, H., van den Born, M., Danenberg, E., Clarke, A.R., Sansom, O.J., and Clevers, H. (2009). Crypt stem cells as the cells-of-origin of intestinal cancer. Nature *457*, 608–611.

Barnes, E.A., Kong, M., Ollendorff, V., and Donoghue, D.J. (2001). Patched1 interacts with cyclin B1 to regulate cell cycle progression. EMBO J. *20*, 2214–2223.

Blanpain, C., and Fuchs, E. (2009). Epidermal homeostasis: a balancing act of stem cells in the skin. Nat. Rev. Mol. Cell Biol. *10*, 207–217.

Blanpain, C., Lowry, W.E., Geoghegan, A., Polak, L., and Fuchs, E. (2004). Self-renewal, multipotency, and the existence of two cell populations within an epithelial stem cell niche. Cell *118*, 635–648.

Chidambaram, A., Goldstein, A.M., Gailani, M.R., Gerrard, B., Bale, S.J., DiGiovanna, J.J., Bale, A.E., and Dean, M. (1996). Mutations in the human homologue of the Drosophila patched gene in Caucasian and African-American nevoid basal cell carcinoma syndrome patients. Cancer Res. *56*, 4599–4601.

Claudinot, S., Nicolas, M., Oshima, H., Rochat, A., and Barrandon, Y. (2005). Long-term renewal of hair follicles from clonogenic multipotent stem cells. Proc. Natl. Acad. Sci. USA *102*, 14677–14682.

Cotsarelis, G., Sun, T.T., and Lavker, R.M. (1990). Label-retaining cells reside in the bulge area of pilosebaceous unit: implications for follicular stem cells, hair cycle, and skin carcinogenesis. Cell *61*, 1329–1337.

Cozzio, A., Passegue, E., Ayton, P.M., Karsunky, H., Cleary, M.L., and Weissman, I.L. (2003). Similar MLL-associated leukemias arising from self-renewing stem cells and short-lived myeloid progenitors. Genes Dev. *17*, 3029–3035.

Dahmane, N., Lee, J., Robins, P., Heller, P., and Ruiz i Altaba, A. (1997). Activation of the transcription factor Gli1 and the Sonic hedgehog signalling pathway in skin tumours. Nature *389*, 876–881.

Donovan, J. (2009). Review of the hair follicle origin hypothesis for basal cell carcinoma. Dermatol. Surg. *35*, 1311–1323.

Epstein, E.H. (2008). Basal cell carcinomas: attack of the hedgehog. Nat. Rev. Cancer *8*, 743–754.

Fazaa, B., Cribier, B., Zaraa, I., Zermani, R., Zeglaoui, F., Zouari, B., Ben Jilani, S., Maalej, M., and Kamoun, M.R. (2007). Low-dose X-ray depilatory treatment induces trichoblastic tumors of the scalp. Dermatology *215*, 301–307.

Flores, I., and Blasco, M.A. (2009). A p53-dependent response limits epidermal stem cell functionality and organismal size in mice with short telomeres. PLoS ONE *4*, e4934.

Gailani, M.R., Leffell, D.J., Ziegler, A., Gross, E.G., Brash, D.E., and Bale, A.E. (1996a). Relationship between sunlight exposure and a key genetic alteration in basal cell carcinoma. J. Natl. Cancer Inst. *88*, 349–354.

Gailani, M.R., Stahle-Backdahl, M., Leffell, D.J., Glynn, M., Zaphiropoulos, P.G., Pressman, C., Unden, A.B., Dean, M., Brash, D.E., Bale, A.E., and Toftgard, R. (1996b). The role of the human homologue of Drosophila patched in sporadic basal cell carcinomas. Nat. Genet. *14*, 78–81.

Ghazizadeh, S., and Taichman, L.B. (2001). Multiple classes of stem cells in cutaneous epithelium: a lineage analysis of adult mouse skin. EMBO J. *20*, 1215–1222.

Goodrich, L.V., Milenkovic, L., Higgins, K.M., and Scott, M.P. (1997). Altered neural cell fates and medulloblastoma in mouse patched mutants. Science *277*, 1109–1113.

Gottlieb, E., and Vousden, K.H. (2010). p53 regulation of metabolic pathways. Cold Spring Harb. Perspect. Biol. *2*, a001040.

Grachtchouk, V., Grachtchouk, M., Lowe, L., Johnson, T., Wei, L., Wang, A., de Sauvage, F., and Dlugosz, A.A. (2003). The magnitude of hedgehog signaling activity defines skin tumor phenotype. EMBO J. *22*, 2741–2751.

Hahn, H., Wicking, C., Zaphiropoulous, P.G., Gailani, M.R., Shanley, S., Chidambaram, A., Vorechovsky, I., Holmberg, E., Unden, A.B., Gillies, S., et al. (1996). Mutations of the human homolog of Drosophila patched in the nevoid basal cell carcinoma syndrome. Cell *85*, 841–851.

Hutchin, M.E., Kariapper, M.S., Grachtchouk, M., Wang, A., Wei, L., Cummings, D., Liu, J., Michael, L.E., Glick, A., and Dlugosz, A.A. (2005). Sustained Hedgehog signaling is required for basal cell carcinoma proliferation and survival: conditional skin tumorigenesis recapitulates the hair growth cycle. Genes Dev. *19*, 214–223.

Indra, A.K., Li, M., Brocard, J., Warot, X., Bornert, J.M., Gerard, C., Messaddeq, N., Chambon, P., and Metzger, D. (2000). Targeted somatic mutagenesis in mouse epidermis. Horm. Res. *54*, 296–300.

Ito, M., Liu, Y., Yang, Z., Nguyen, J., Liang, F., Morris, R.J., and Cotsarelis, G. (2005). Stem cells in the hair follicle bulge contribute to wound repair but not to homeostasis of the epidermis. Nat. Med. *11*, 1351–1354.

Jaks, V., Barker, N., Kasper, M., van Es, J.H., Snippert, H.J., Clevers, H., and Toftgard, R. (2008). Lgr5 marks cycling, yet long-lived, hair follicle stem cells. Nat. Genet. *40*, 1291–1299.

Johnson, R.L., Rothman, A.L., Xie, J., Goodrich, L.V., Bare, J.W., Bonifas, J.M., Quinn, A.G., Myers, R.M., Cox, D.R., Epstein, E.H., Jr., and Scott, M.P. (1996). Human homolog of patched, a candidate gene for the basal cell nevus syndrome. Science *272*, 1668–1671.

Jonkers, J., Meuwissen, R., van der Gulden, H., Peterse, H., van der Valk, M., and Berns, A. (2001). Synergistic tumor suppressor activity of BRCA2 and p53 in a conditional mouse model for breast cancer. Nat. Genet. *29*, 418–425.

Kawamura, T., Suzuki, J., Wang, Y.V., Menendez, S., Morera, L.B., Raya, A., Wahl, G.M., and Belmonte, J.C. (2009). Linking the p53 tumour suppressor pathway to somatic cell reprogramming. Nature *460*, 1140–1144.

Langton, A.K., Herrick, S.E., and Headon, D.J. (2008). An extended epidermal response heals cutaneous wounds in the absence of a hair follicle stem cell contribution. J. Invest. Dermatol. *128*, 1311–1318.

Le, L.Q., Shipman, T., Burns, D.K., and Parada, L.F. (2009). Cell of origin and microenvironment contribution for NF1-associated dermal neurofibromas. Cell Stem Cell *4*, 453–463.

Lench, N.J., Telford, E.A., High, A.S., Markham, A.F., Wicking, C., and Wainwright, B.J. (1997). Characterisation of human patched germ line mutations in naevoid basal cell carcinoma syndrome. Hum. Genet. *100*, 497–502.

Levy, V., Lindon, C., Harfe, B.D., and Morgan, B.A. (2005). Distinct stem cell populations regenerate the follicle and interfollicular epidermis. Dev. Cell *9*, 855–861.

Ling, G., Ahmadian, A., Persson, A., Unden, A.B., Afink, G., Williams, C., Uhlen, M., Toftgard, R., Lundeberg, J., and Ponten, F. (2001). PATCHED and p53 gene alterations in sporadic and hereditary basal cell cancer. Oncogene *20*, 7770–7778.

Liu, Y., Lyle, S., Yang, Z., and Cotsarelis, G. (2003). Keratin 15 promoter targets putative epithelial stem cells in the hair follicle bulge. J. Invest. Dermatol. *121*, 963–968.

Mancuso, M., Leonardi, S., Tanori, M., Pasquali, E., Pierdomenico, M., Rebessi, S., Di Majo, V., Covelli, V., Pazzaglia, S., and Saran, A. (2006). Hair cycle-dependent basal cell carcinoma tumorigenesis in Ptc1neo67/+ mice exposed to radiation. Cancer Res. *66*, 6606–6614.

Mancuso, M., Pazzaglia, S., Tanori, M., Hahn, H., Merola, P., Rebessi, S., Atkinson, M.J., Di Majo, V., Covelli, V., and Saran, A. (2004). Basal cell carcinoma and its development: insights from radiation-induced tumors in Ptch1-deficient mice. Cancer Res. *64*, 934–941.

Meletis, K., Wirta, V., Hede, S.M., Nister, M., Lundeberg, J., and Frisen, J. (2006). p53 suppresses the self-renewal of adult neural stem cells. Development *133*, 363–369.

Milenkovic, L., Goodrich, L.V., Higgins, K.M., and Scott, M.P. (1999). Mouse patched1 controls body size determination and limb patterning. Development *126*, 4431–4440.

Morris, R.J. (2000). Keratinocyte stem cells: targets for cutaneous carcinogens. J. Clin. Invest. *106*, 3–8.

Morris, R.J., and Potten, C.S. (1999). Highly persistent label-retaining cells in the hair follicles of mice and their fate following induction of anagen. J. Invest. Dermatol. *112*, 470–475.

Morris, R.J., Liu, Y., Marles, L., Yang, Z., Trempus, C., Li, S., Lin, J.S., Sawicki, J.A., and Cotsarelis, G. (2004). Capturing and profiling adult hair follicle stem cells. Nat. Biotechnol. *22*, 411–417.

Nilsson, M., Unden, A.B., Krause, D., Malmqwist, U., Raza, K., Zaphiropoulos, P.G., and Toftgard, R. (2000). Induction of basal cell carcinomas and trichoepitheliomas in mice overexpressing GLI-1. Proc. Natl. Acad. Sci. USA *97*, 3438–3443.

Oro, A.E., Higgins, K.M., Hu, Z., Bonifas, J.M., Epstein, E.H., Jr., and Scott, M.P. (1997). Basal cell carcinomas in mice overexpressing sonic hedgehog. Science *276*, 817–821.

Perez-Losada, J., and Balmain, A. (2003). Stem-cell hierarchy in skin cancer. Nat. Rev. Cancer *3*, 434–443.

Rady, P., Scinicariello, F., Wagner, R.F., Jr., and Tyring, S.K. (1992). p53 mutations in basal cell carcinomas. Cancer Res. *52*, 3804–3806.

Reifenberger, J., Wolter, M., Knobbe, C.B., Kohler, B., Schonicke, A., Scharwachter, C., Kumar, K., Blaschke, B., Ruzicka, T., and Reifenberger, G. (2005). Somatic mutations in the PTCH, SMOH, SUFUH and TP53 genes in sporadic basal cell carcinomas. Br. J. Dermatol. *152*, 43–51.

Ridky, T.W., and Khavari, P.A. (2010). The hair follicle bulge stem cell niche resists transformation by the hedgehog pathway. Cell Stem Cell *6*, 292–294.

Sato, T., Vries, R.G., Snippert, H.J., van de Wetering, M., Barker, N., Stange, D.E., van Es, J.H., Abo, A., Kujala, P., Peters, P.J., and Clevers, H. (2009). Single Lgr5 stem cells build crypt-villus structures in vitro without a mesenchymal niche. Nature *459*, 262–265.

Scales, S.J., and de Sauvage, F.J. (2009). Mechanisms of Hedgehog pathway activation in cancer and implications for therapy. Trends Pharmacol. Sci. *30*, 303–312.

Schuller, U., Heine, V.M., Mao, J., Kho, A.T., Dillon, A.K., Han, Y.G., Huillard, E., Sun, T., Ligon, A.H., Qian, Y., et al. (2008). Acquisition of granule neuron precursor identity is a critical determinant of progenitor cell competence to form Shh-induced medulloblastoma. Cancer Cell *14*, 123–134.

Snippert, H.J., Haegebarth, A., Kasper, M., Jaks, V., van Es, J.H., Barker, N., van de Wetering, M., van den Born, M., Begthel, H., Vries, R.G., et al. (2010). Lgr6 marks stem cells in the hair follicle that generate all cell lineages of the skin. Science *327*, 1385–1389.

Srinivas, S., Watanabe, T., Lin, C.S., William, C.M., Tanabe, Y., Jessell, T.M., and Costantini, F. (2001). Cre reporter strains produced by targeted insertion of EYFP and ECFP into the ROSA26 locus. BMC Dev. Biol. *1*, 4.

Svard, J., Heby-Henricson, K., Persson-Lek, M., Rozell, B., Lauth, M., Bergstrom, A., Ericson, J., Toftgard, R., and Teglund, S. (2006). Genetic elimination of Suppressor of fused reveals an essential repressor function in the mammalian Hedgehog signaling pathway. Dev. Cell *10*, 187–197.

Taylor, G., Lehrer, M.S., Jensen, P.J., Sun, T.T., and Lavker, R.M. (2000). Involvement of follicular stem cells in forming not only the follicle but also the epidermis. Cell *102*, 451–461.

Trempus, C.S., Morris, R.J., Bortner, C.D., Cotsarelis, G., Faircloth, R.S., Reece, J.M., and Tennant, R.W. (2003). Enrichment for living murine keratinocytes from the hair follicle bulge with the cell surface marker CD34. J. Invest. Dermatol. *120*, 501–511.

Tumbar, T., Guasch, G., Greco, V., Blanpain, C., Lowry, W.E., Rendl, M., and Fuchs, E. (2004). Defining the epithelial stem cell niche in skin. Science *303*, 359–363.

Unden, A.B., Holmberg, E., Lundh-Rozell, B., Stahle-Backdahl, M., Zaphiropoulos, P.G., Toftgard, R., and Vorechovsky, I. (1996). Mutations in the human homologue of Drosophila patched (PTCH) in basal cell carcinomas and the Gorlin syndrome: different in vivo mechanisms of PTCH inactivation. Cancer Res. *56*, 4562–4565.

Vousden, K.H., and Ryan, K.M. (2009). p53 and metabolism. Nat. Rev. Cancer *9*, 691–700.

Walter, K., Omura, N., Hong, S.M., Griffith, M., Vincent, A., Borges, M., and Goggins, M. (2010). Overexpression of smoothened activates the sonic hedgehog signaling pathway in pancreatic cancer-associated fibroblasts. Clin. Cancer Res. *16*, 1781–1789.

Wang, X., Kruithof-de Julio, M., Economides, K.D., Walker, D., Yu, H., Halili, M.V., Hu, Y.P., Price, S.M., Abate-Shen, C., and Shen, M.M. (2009). A luminal epithelial stem cell that is a cell of origin for prostate cancer. Nature *461*, 495–500.

Watt, F.M., and Jensen, K.B. (2009). Epidermal stem cell diversity and quiescence. EMBO Mol. Med. *1*, 260–267.

Wetmore, C., Eberhart, D.E., and Curran, T. (2001). Loss of p53 but not ARF accelerates medulloblastoma in mice heterozygous for patched. Cancer Res. *61*, 513–516.

Wicking, C., Shanley, S., Smyth, I., Gillies, S., Negus, K., Graham, S., Suthers, G., Haites, N., Edwards, M., Wainwright, B., and Chenevix-Trench, G. (1997). Most germ-line mutations in the nevoid basal cell carcinoma syndrome lead to a premature termination of the PATCHED protein, and no genotype-phenotype correlations are evident. Am. J. Hum. Genet. *60*, 21–26.

Wolter, M., Reifenberger, J., Sommer, C., Ruzicka, T., and Reifenberger, G. (1997). Mutations in the human homologue of the Drosophila segment polarity gene patched (PTCH) in sporadic basal cell carcinomas of the skin and primitive neuroectodermal tumors of the central nervous system. Cancer Res. *57*, 2581–2585.

Yang, Z.J., Ellis, T., Markant, S.L., Read, T.A., Kessler, J.D., Bourboulas, M., Schuller, U., Machold, R., Fishell, G., Rowitch, D.H., et al. (2008). Medulloblastoma can be initiated by deletion of Patched in lineage-restricted progenitors or stem cells. Cancer Cell *14*, 135–145.

Youssef, K.K., Van Keymeulen, A., Lapouge, G., Beck, B., Michaux, C., Achouri, Y., Sotiropoulou, P.A., and Blanpain, C. (2010). Identification of the cell lineage at the origin of basal cell carcinoma. Nat. Cell Biol. *12*, 299–305.

Zhao, C., Chen, A., Jamieson, C.H., Fereshteh, M., Abrahamsson, A., Blum, J., Kwon, H.Y., Kim, J., Chute, J.P., Rizzieri, D., et al. (2009). Hedgehog signalling is essential for maintenance of cancer stem cells in myeloid leukaemia. Nature *458*, 776–779.

Ziegler, A., Jonason, A.S., Leffell, D.J., Simon, J.A., Sharma, H.W., Kimmelman, J., Remington, L., Jacks, T., and Brash, D.E. (1994). Sunburn and p53 in the onset of skin cancer. Nature *372*, 773–776.